

# Revisiting the Signature Extraction from Low-Band 1 Data using MCMC

Raul A. Monsalve  
[raul.monsalve@colorado.edu](mailto:raul.monsalve@colorado.edu)

CASA, University of Colorado Boulder  
 SESE, Arizona State University

September 25, 2017

Here, we compare results for the signature extraction from Low-Band 1 data with extended ground plane (CASE 2), when using the traditional SNR search and a Markov-Chain Monte Carlo (MCMC) algorithm.

The MCMC approach was first attempted in report #93. Here we apply the MCMC approach again but using a better integrated spectrum (better calibrated and RFI-cleaned). The dataset used to generate the spectrum, as well as the calibration details, are the same as those shown in report #106. They are the following:

- Dates: 2016-258 to 2017-95
- Sun cut: none
- Moon cut: none
- Receiver calibration S11 file: `s11_calibration_low_band_LNA25degC_2015-09-16-12-30-29_simulator2_long.txt`
- Receiver parameter polynomial terms:  $N_{\text{fit}}=6$ ,  $W_{\text{fit}}=5$
- Antenna S11 file: `S11_blade_low_band_2016_243.txt`
- Antenna S11 modeling: 9 polynomial terms after removal of delay
- Balun loss correction: yes
- Ground loss correction: yes, 0.5%
- Beam correction: yes, using beam file *newniv* rotated to  $AZ = -7^\circ$ , and Haslam sky map scaled to 76 MHz using  $\beta = -2.5$ .

The MCMC approach fits simultaneously all the nonlinear parameters of the phenomenological model for the absorption signature (described in report #93), in addition to the foreground coefficients. This enables us to obtain uncertainties on the parameters that account for all their covariances.

The nominal analysis consists of a fit to the range 60-94 MHz with 5 terms of the EDGES polynomial. For the 21-cm model, the fit considers initially three parameters:  $a_{21}$ ,  $\nu_r$ , and  $\Delta\nu$ , with  $\tau = 7$  and  $\chi = 0$  fixed. But in two other cases we incorporate  $\tau$  and  $\chi$  into the fit. In the MCMC approach, the Gaussian noise assumed has a frequency-independent standard deviation of 13 mK. We used this value because it is close to the typical RMS of the residuals to the best-fit model. Also, the total number of MCMC samples employed is sufficient to thoroughly map the parameter posteriors, after removing samples that correspond to the burn in period. The rest of the report contains the following tables and figures:

- Table 1 compares the results from the SNR search and the MCMC fit.
- Table 2 compares the results for the MCMC approach assuming two values for the (frequency-independent) noise standard deviations: 13 (nominal), and 20 mK. This is done to quantify the sensitivity of the parameter uncertainties to the assumed noise level.
- Figure 1 compares the best fits for the signatures from the two methods. It also shows a random sample of 200 models probed during the MCMC exploration.
- Figure 2 shows the posterior distributions for the MCMC case with 3 fit parameters for the 21-cm model ( $a_{21}$ ,  $\nu_r$ , and  $\Delta\nu$ ).
- Figure 3 shows the posterior distributions for the MCMC case with 4 fit parameters for the 21-cm model ( $a_{21}$ ,  $\nu_r$ ,  $\Delta\nu$ , and  $\tau$ ).
- Figure 4 shows the posterior distributions for the MCMC case with 5 fit parameters for the 21-cm model ( $a_{21}$ ,  $\nu_r$ ,  $\Delta\nu$ ,  $\tau$ , and  $\chi$ ).
- Figure 5 shows the residuals to the best fits for both fitting methods, as well as for the three cases that consider 3, 4, and 5 fit parameters in the 21-cm model.
- Figure 6 shows histograms for the distributions of the residual RMS from the MCMC fits, for the two noise levels assumed.

## Conclusions

1. Even though the figure of merit is not the same in both methods (SNR vs  $\chi^2$  statistic), the agreement between the best-fit models is good.
2. In principle, the uncertainty of  $a_{21}$  derived from the SNR grid search does not consider covariance between this and the other 21-cm parameters, while covariance is considered in the MCMC approach. When the only parameters in the fit are  $a_{21}$ ,  $\nu_r$ , and  $\Delta\nu$ , the uncertainty of  $a_{21}$  from the MCMC is about the same as in the grid search ( $\sim 20$  mK). This shows that the covariance between  $a_{21}$ , and  $\nu_r$  and  $\Delta\nu$ , is small, and that the grid search, as implemented, produces adequate uncertainties for  $a_{21}$ . Therefore, the signature SNR computed from the grid search is also adequate.
3. When the two additional 21-cm parameters ( $\tau$  and  $\chi$ ) are incorporated into the MCMC fit, the uncertainties in  $a_{21}$  grow, while the uncertainties in  $\nu_r$  and  $\Delta\nu$  stay about the same. The most significant increase in the  $a_{21}$  uncertainty occurs when  $\tau$  is added to the fit, while keeping the tilt fixed. For an assumed noise standard deviation of 13 mK, the best-fit estimate and 68% uncertainties go from  $494_{-21}^{+21}$  mK ( $\tau = 7$ ,  $\chi = 0$ ) to  $524_{-78}^{+111}$  mK ( $\tau$  in the fit,  $\chi = 0$ ).

4. The residuals to the fit of the absorption signature suggest that the 21-cm model is not complete without incorporating the tilt in the fit. Adding the tilt to the fit results in almost noise-like best-fit residuals (RMS of 10 mK for the nominal case). The best-fit tilt value is  $\sim -0.47$ . However, without careful comparisons, this tilt value has to be considered specific to the integrated spectrum used for this report, and not necessarily applicable to, or consistent with, other Low-Band spectra. More work is necessary to determine if this tilt value represents a true feature in the signature.

Table 1: Comparison between SNR search and MCMC, for 3, 4, and 5 fit parameters of the 21-cm model. In all cases, the fit is done with 5 terms of the EDGES polynomial, and over 60-94 MHz. The noise standard deviation is 13 mK. The uncertainties represent 68% limits. Red numbers represent fixed values.

Approach	$a_{21}$ [mK]	$\nu_r$ [MHz]	$\Delta\nu$ [MHz]	$\tau$	$\chi$
SNR search	$514^{+20}_{-20}$	78.2	20.5	7	0
MCMC	$494^{+21}_{-21}$	$78.25^{+0.08}_{-0.08}$	$20.64^{+0.19}_{-0.19}$	7	0
SNR search	$588^{+23}_{-23}$	78.3	20.7	6.0	0
MCMC	$524^{+111}_{-78}$	$78.27^{+0.09}_{-0.09}$	$20.71^{+0.29}_{-0.26}$	$6.51^{+1.49}_{-1.21}$	0
SNR search	$570^{+18}_{-18}$	78.1	20.0	5.8	-0.5
MCMC	$568^{+151}_{-102}$	$78.11^{+0.09}_{-0.09}$	$20.03^{+0.24}_{-0.24}$	$5.84^{+1.59}_{-1.18}$	$-0.47^{+0.07}_{-0.07}$

Table 2: Results for MCMC approach with two different noise levels. The uncertainties represent 68% limits. Red numbers represent fixed values.

noise std dev [mK]	$a_{21}$ [mK]	$\nu_r$ [MHz]	$\Delta\nu$ [MHz]	$\tau$	$\chi$
13 (nominal)	$494^{+21}_{-21}$	$78.25^{+0.08}_{-0.08}$	$20.64^{+0.19}_{-0.19}$	7	0
20	$495^{+34}_{-34}$	$78.25^{+0.13}_{-0.13}$	$20.64^{+0.3}_{-0.28}$	7	0
13 (nominal)	$524^{+111}_{-78}$	$78.27^{+0.09}_{-0.09}$	$20.71^{+0.29}_{-0.26}$	$6.51^{+1.49}_{-1.21}$	0
20	$504^{+157}_{-102}$	$78.26^{+0.14}_{-0.13}$	$20.67^{+0.42}_{-0.38}$	$6.77^{+2.54}_{-1.64}$	0
13 (nominal)	$568^{+151}_{-102}$	$78.11^{+0.09}_{-0.09}$	$20.03^{+0.24}_{-0.24}$	$5.84^{+1.59}_{-1.18}$	$-0.47^{+0.07}_{-0.07}$
20	$545^{+223}_{-139}$	$78.12^{+0.14}_{-0.14}$	$20.06^{+0.4}_{-0.37}$	$6.08^{+2.99}_{-1.68}$	$-0.46^{+0.12}_{-0.11}$

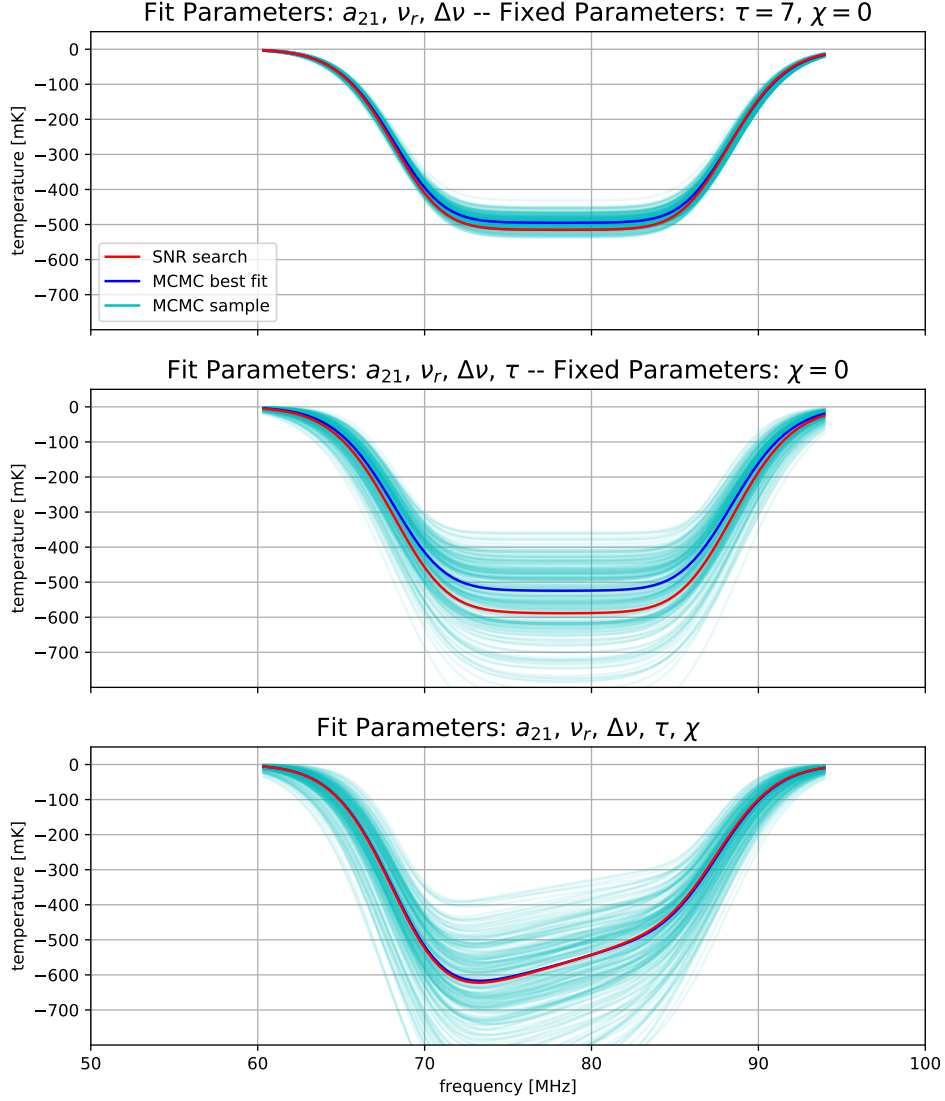


Figure 1: Best fit 21-cm signature from the SNR grid search and the MCMC method. The top panel corresponds to a 21-cm with three fit parameters:  $a_{21}, \nu_r,$  and  $\Delta\nu$ , with  $\tau = 7$  and  $\chi = 0$  fixed. In the middle panel, the flattening parameter  $\tau$  is added to the fit. In the bottom panel, the tilt parameter  $\chi$  is added to the fit. When the flattening parameter is added to the fit, the MCMC estimates  $\tau = 6.77^{+2.54}_{-1.64}$ , which is similar to  $\tau = 7$  assumed in the top panel. When the tilt parameter is added to the fit, the MCMC estimates  $\chi = -0.46^{+0.12}_{-0.11}$ , which is significantly different from  $\chi = 0$  assumed in the top and middle panels. It cannot be assumed that this value of tilt is consistent with integrated spectra from other low-band datasets.

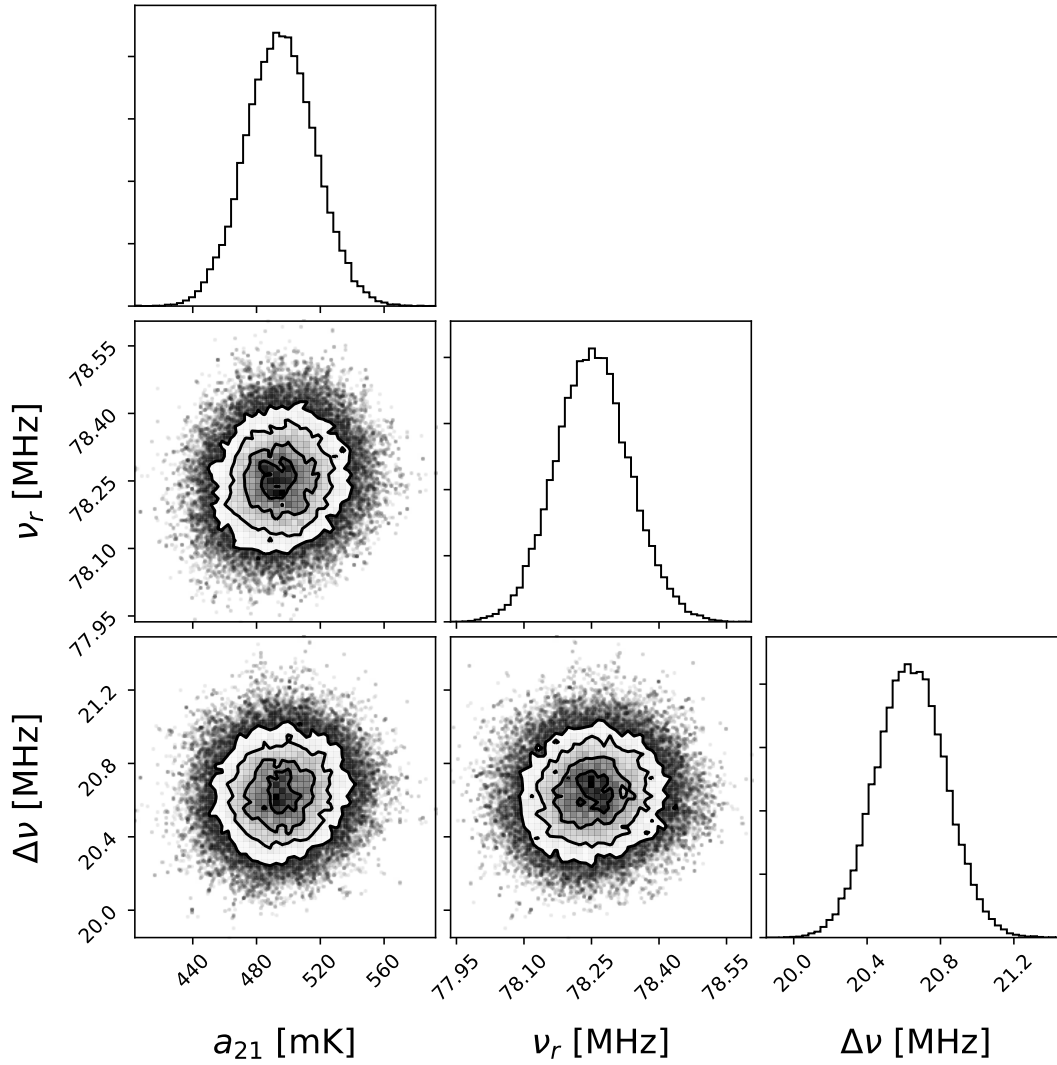


Figure 2: MCMC posterior distributions when using 3 fit parameters for the 21-cm model ( $a_{21}$ ,  $\nu_r$ , and  $\Delta\nu$ ). The distributions account for covariances with the 5 foreground terms.

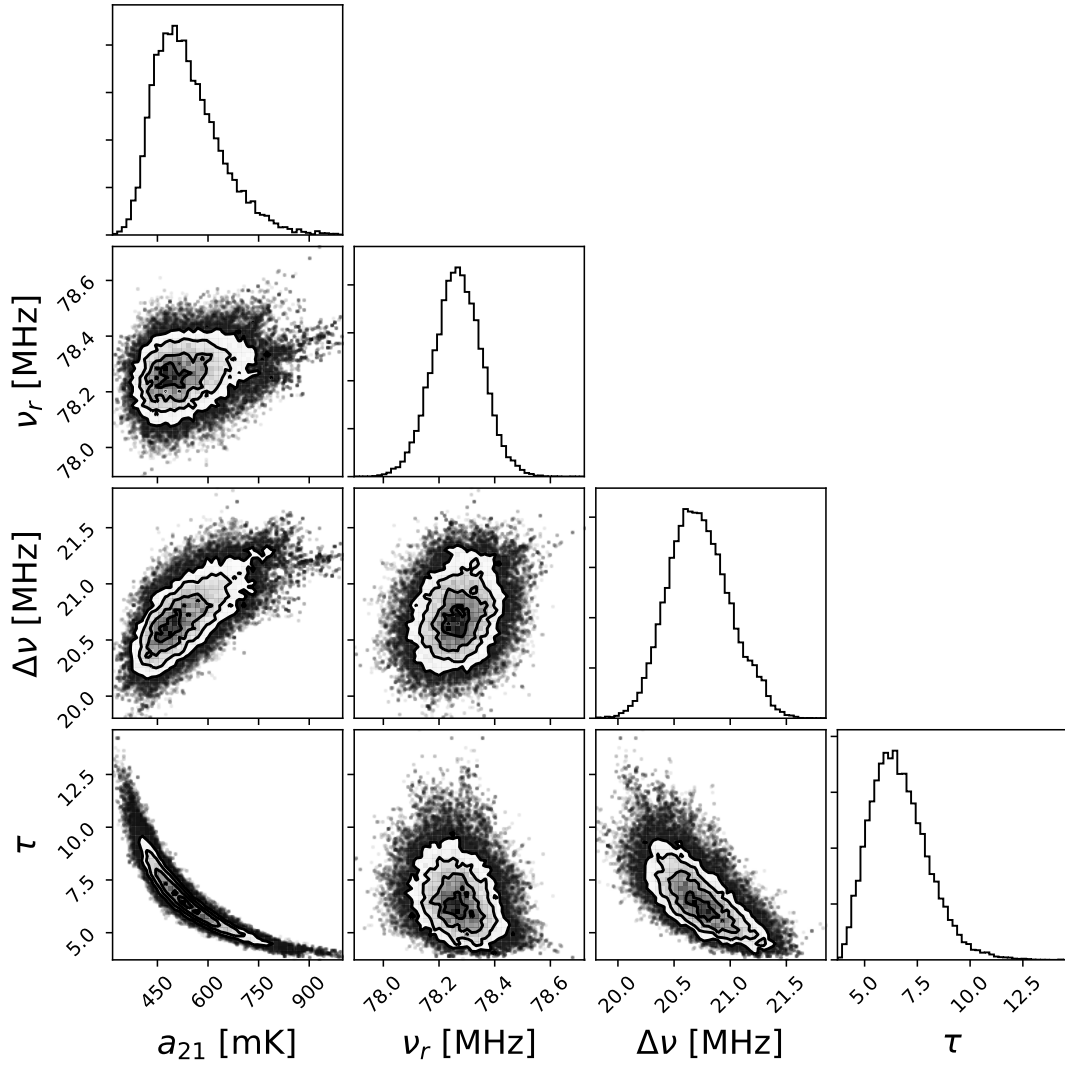


Figure 3: MCMC posterior distributions when using 4 fit parameters for the 21-cm model ( $a_{21}$ ,  $\nu_r$ ,  $\Delta\nu$ , and  $\tau$ ). The distributions account for covariances with the 5 foreground terms.

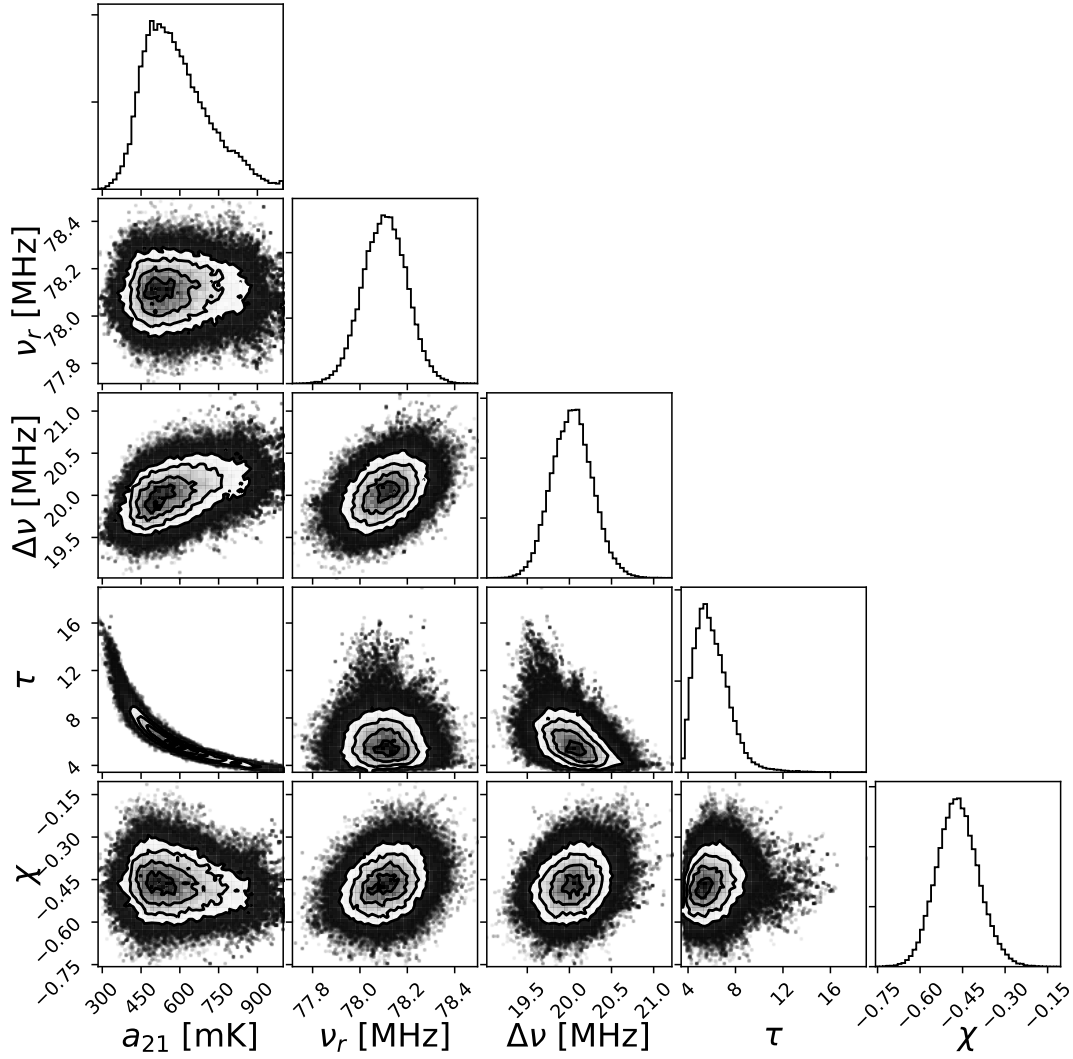


Figure 4: MCMC posterior distributions when using 5 fit parameters for the 21-cm model ( $a_{21}$ ,  $\nu_r$ ,  $\Delta\nu$ ,  $\tau$ , and  $\chi$ ). The distributions account for covariances with the 5 foreground terms.

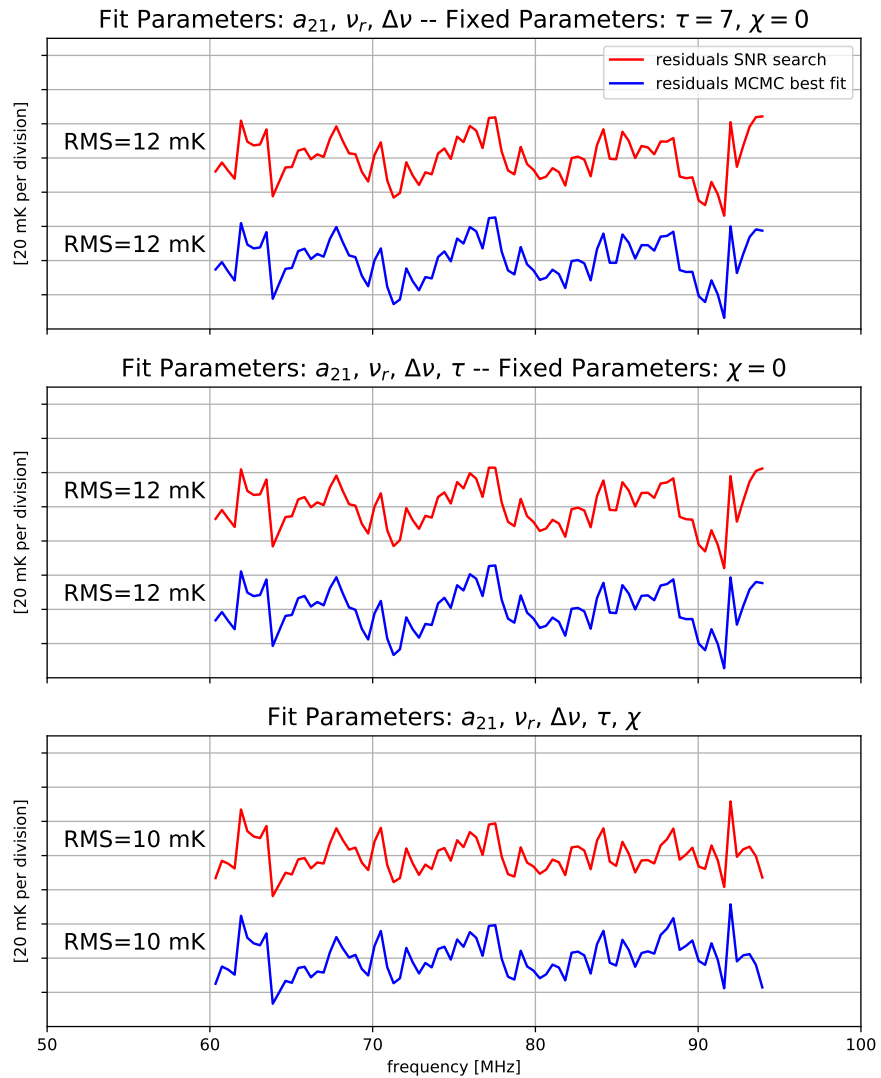


Figure 5: Residuals to the best fit models obtained by the SNR grid search and the MCMC method. The bottom panel shows that incorporating the  $\chi$  tilt parameter to the fit, instead of fixing it at  $\chi = 0$ , reduces the residuals.

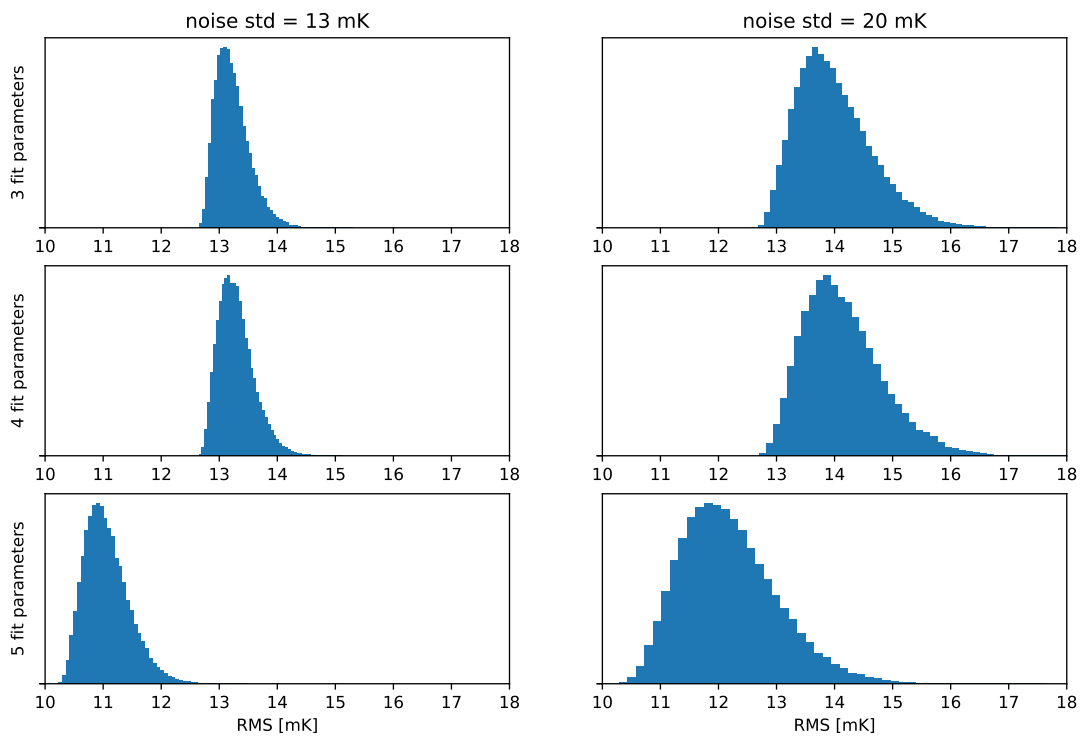


Figure 6: Distributions of residual RMS for the MCMC cases with 3, 4, and 5 21-cm parameters (rows) and two noise levels (columns). Including the  $\chi$  tilt parameters in the fit (lowest row) reduces the typical residuals.